

## Supporting Information

### **An Organodiselenide Containing Electrolyte Enable Sulfurized Polyacrylonitrile Cathodes with Fast Redox Kinetics in Li-S batteries**

Wei Zhang<sup>a</sup>, Qiang Wu<sup>b</sup>, Ziqi Zeng<sup>a</sup>, Chuang Yu<sup>a</sup>, Shijie Cheng<sup>a</sup> and Jia Xie<sup>\*a</sup>

<sup>a</sup>State Key Laboratory of Advanced Electromagnetic Engineering and Technology, School of Electrical and Electronic Engineering, Huazhong University of Science and Technology, Wuhan 430074, P. R. China.

<sup>b</sup>State Key Laboratory of Materials Processing and Die & Mould Technology, School of Materials Science and Engineering, Huazhong University of Science and Technology, Wuhan, 430074, China

\*Correspondence to: [xiejia@hust.edu.cn](mailto:xiejia@hust.edu.cn)

---

## 1. Experimental section

### 1.1. Raw materials

1,3-dioxolane (DOL), 1,2-dimethoxyethane (DME), lithium nitrate ( $\text{LiNO}_3$ ), Polyacrylonitrile (PAN,  $M_w=150,000$ ), sulfur ( $\text{S}_8$ ) and Carboxymethyl cellulose (CMC) were purchased from Sigma-Aldrich. The ethylene carbonate (EC), diethyl carbonate (DEC), fluoroethylene carbonate (FEC), Li bis(trifluoromethanesulfonyl)imide (LiTFSI), and lithium hexafluorophosphate ( $\text{LiPF}_6$ ) were purchased from Guangzhou Tinci Materials Technology Co., Ltd. Lithium (Li) metal foils (400  $\mu\text{m}$  in thickness, 16.0 mm in diameter) were purchased from Guangdong Canrd New Energy Technology Co., Ltd. The aluminum (Al) foil and Celgard 2400 polypropylene (PP) membranes were provided by Shenzhen Kejing Star Technology Co., Ltd. Ketjen black (KB) was from Lion Corp., Japan. Diphenyl diselenide (PDSe) and styrene butadiene rubber (SBR) were purchased from Shanghai Macklin Biochemical Co., Ltd. The commercial binder-free carbon nanotube paper called buckypaper (NanoTechLabs, Inc) was used as the current collector in this study. The carbon paper was cut into 0.5  $\text{cm}^2$  discs ( $D = 8 \text{ mm}$ ) and dried at 100  $^\circ\text{C}$  for 24 h in a vacuum oven before use.

### 1.2. Synthesis of SPAN

S@pPAN composites were synthesized through a milling and calcination method, according to previously reported work <sup>[1-2]</sup>. Briefly, sulfur powder and PAN powder were firstly mixed with a weight ratio of 3:1 and ball milled for 1h under 400 rpm. Then, the obtained mixture was annealed at 300  $^\circ\text{C}$  for 3 h in Ar atmosphere. Excess amount of S were removed in the dehydrogenation reaction. S@pPAN was obtained after the furnace was cooled to room temperature.

### 1.3. Materials Characterization

---

X-ray diffraction (XRD) was performed to confirm the purity of samples by PANalytical X'pert PRO-DY2198 with Cu K $\alpha$  radiation. Scanning electron microscope (SEM, Sirion200) and Transmission electron microscopy (TEM) (Talos F200X) were employed to probe the microstructures of the as-prepared S@pPAN composites. An energy-dispersive X-ray (EDX) analyzer coupled with TEM was used to determine the chemical compositions of the S@pPAN composites. Raman spectra was performed by LabRAM HR800 (Horiba Jobin Yvon) with laser power 5 mW, wavelength 532 nm and exposure time 10 s. Fourier transform infrared spectra (FT-IR) was taken using a Bruker Vertex 70 FTIR spectrometer. X-ray photoelectron spectroscopy (XPS) measurements was performed by VG MultiLab 2000 system (Thermo VG Scientific) with the samples cleaned with argon plasma in advance. All XPS spectra were calibrated using carbon 1s line at 284.6 eV. The element contents of samples were convinced by elemental analysis on a Vario Micro Cube. GC-MS were analyzed with an Agilent 7890A gas chromatograph coupled to an Agilent 5975C mass spectrometer.

#### *1.4. Electrochemical measurements*

2032 coin cells assembled in an argon-filled glove box ( $\text{H}_2\text{O}$ ,  $\text{O}_2 < 1$  ppm) were used to evaluate the electrochemical performance with lithium foil as the anode. The cathode electrode was prepared by mixing S@pPAN composites, Ketjen black (KB), sodium carboxyl methyl cellulose (NaCMC), and styrene butadiene rubber (SBR) with a weight ratio of 80:10:5:5, in which the active sulfur loading is about  $1.5 \text{ mg cm}^{-2}$ . The slurry was coated onto Al foil and then dried in a vacuum oven at  $80 \text{ }^\circ\text{C}$  for 12 h. Ether and carbonate-based electrolytes were used to test the battery performance of S@pPAN in this work. The ether electrolyte was 1.0 M LiTFSI in a mixture of 1,2-dimethoxyethane (DME) and 1,3-dioxolane (DOL) 1:1 (vol%), containing 2 wt %  $\text{LiNO}_3$ . The carbonate electrolyte was 1.0 M  $\text{LiPF}_6$  in a

---

mixture of ethylene carbonate (EC) and diethyl carbonate (DEC) 1:1 (vol %), with 10 vol % fluoroethylene carbonate (FEC). For the electrolyte with PDSe, the concentration of PDSe is calculated based on the molar ratio of S in S@pPAN to Se in PDSe, differing from 15:1 to 4:1 in both carbonate and ether-based electrolytes.

For the assembling of PDSe-assisted S@pPAN batteries, the prepared S@pPAN cathodes, Li metal foil anodes, and PP separators were assembled into standard 2032 coin cells. The catholyte was 15  $\mu\text{L}$  carbonate or ether-based electrolyte with PDSe, while the anolyte was 20  $\mu\text{L}$  carbonate or ether-based electrolyte without PDSe. S@pPAN batteries were assembled without the addition of PDSe. To test the electrochemical behavior of PDSe, 30  $\mu\text{L}$  1M PDSe in the blank catholyte was dropped onto carbon paper, and 10  $\mu\text{L}$  blank electrolyte was added in the anode.

Galvanostatic charge/discharge profiles were obtained by the battery test system (LAND-CT2001A, Wuhan, China). The electrochemical workstation (Solartron 1470E) was used to test cyclic voltammetry (CV) profiles at a scan rate of 0.01  $\text{mV s}^{-1}$  between 1 and 3 V at room temperature. Galvanostatic intermittent titration technique (GITT) test was performed on Land battery test system, discharging at a current of 100  $\text{mA g}^{-1}$  for 1 h and resting for 4 h. The charging process was tested under the similar program. The mass specific capacities of the S@pPAN composites were calculated based on the mass of S. Lithium ion diffusion coefficients for S@pPAN with/without DPDSe samples were calculated by a series of cyclic voltammograms with different scan rates, and the results were analyzed based on Randles-Sevick equation:  $I_p = 2.69 \times 10^5 n^{1.5} A D_{\text{Li}^+}^{0.5} C_{\text{Li}^+} v^{0.5}$ , in which  $I_p$  represented the peak current (A),  $D_{\text{Li}^+}$  stood for lithium ion diffusion coefficient ( $\text{cm}^2 \text{s}^{-1}$ ),  $n$  was the number of electrons involved in the reaction ( $n = 2$  for Li-S battery),  $A$  referred to the geometric area of the active electrode ( $\text{cm}^2$ ),  $C_{\text{Li}^+}$  represented the lithium ion concentration ( $\text{mol L}^{-1}$ ) and  $v$  stands for scanning rate ( $\text{V s}^{-1}$ ).

## 2. Supplementary Figures and Tables

**Table S1** Elemental analysis of S@pPAN.

Material	C (wt %)	N (wt %)	S (wt %)
S@pPAN	42.35	14.82	42.01

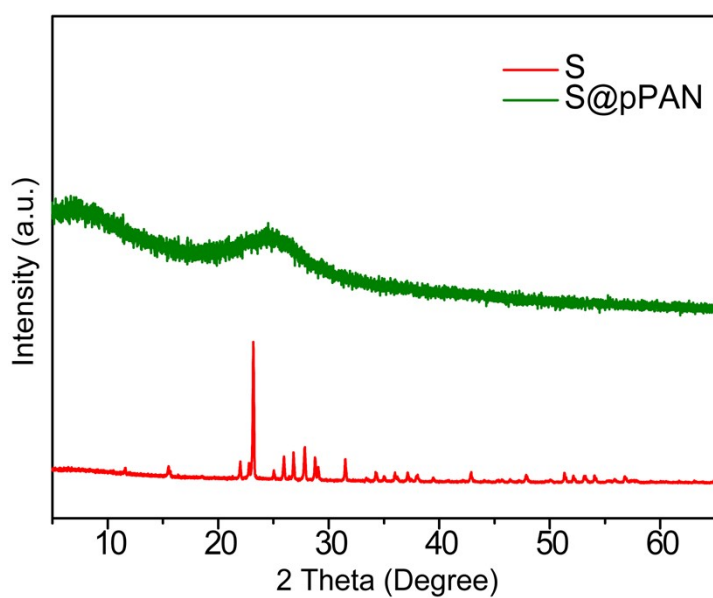


**Fig. S1.** XRD patterns of S powder and S@pPAN.

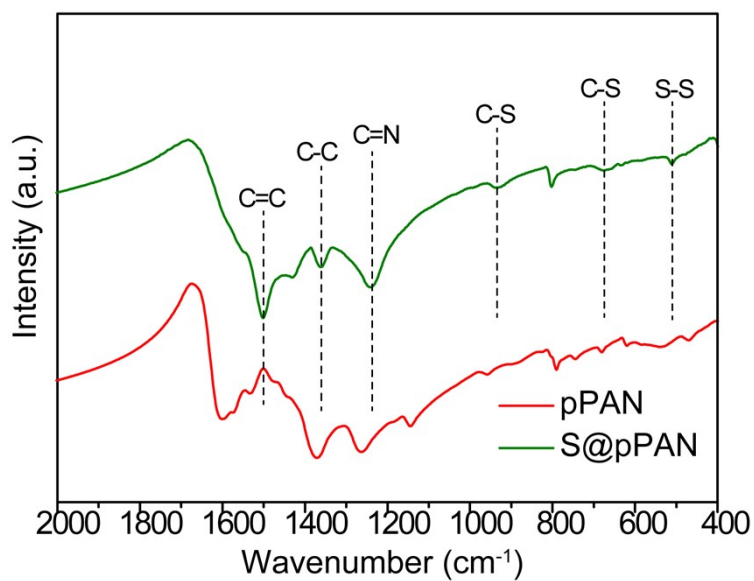


**Fig. S2.** FT-IR spectras of S@pPAN.

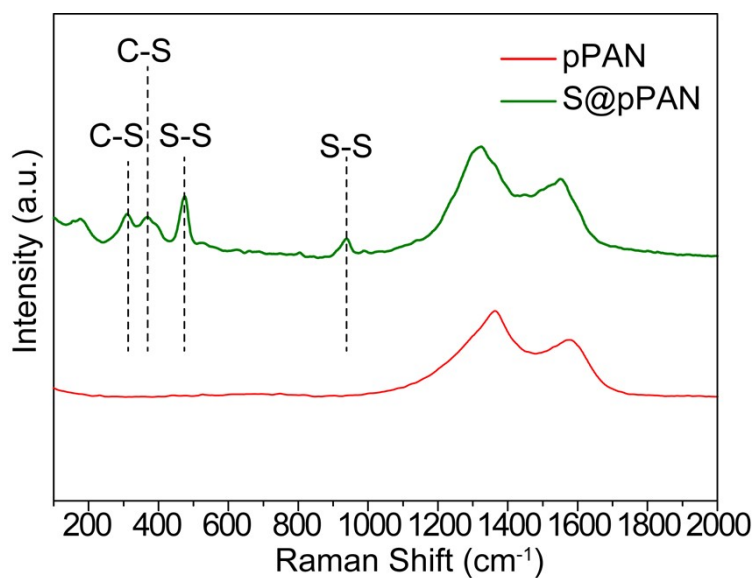


**Fig. S3.** Raman spectras of S@pPAN.

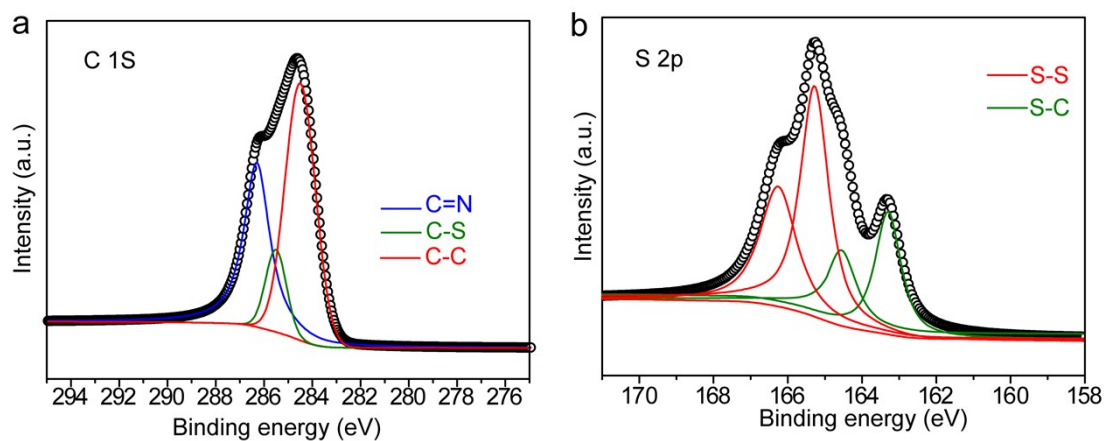


**Fig. S4.** (a) The C 1s and (b) S 2p high-resolution XPS of S@pPAN.

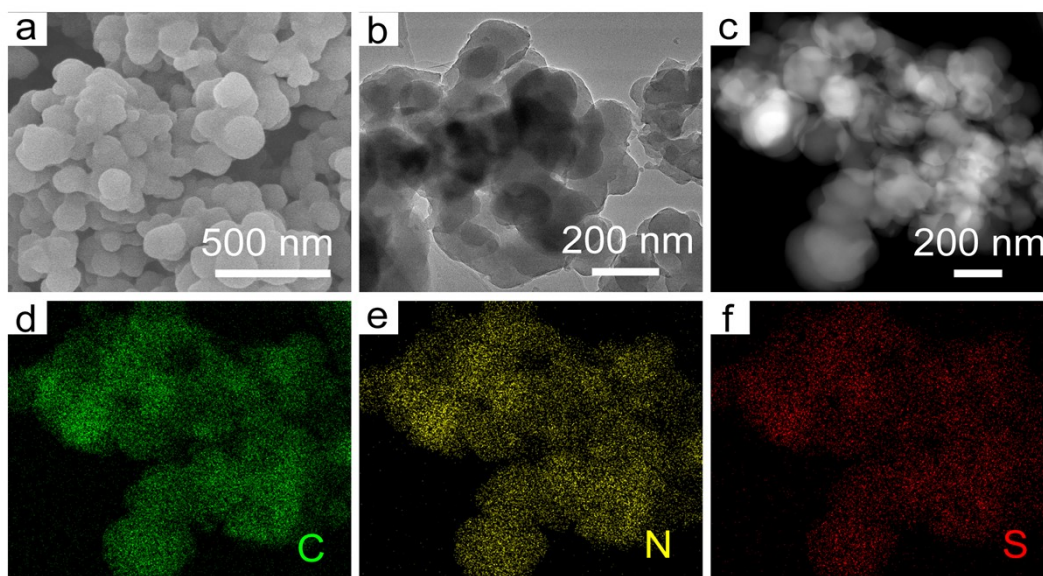


**Fig. S5.** Morphology characterization of S@pPAN. (a) SEM; (b) HR-TEM; (c-f) EDS elemental mapping images for carbon (d), nitrogen (e), and sulfur (f).

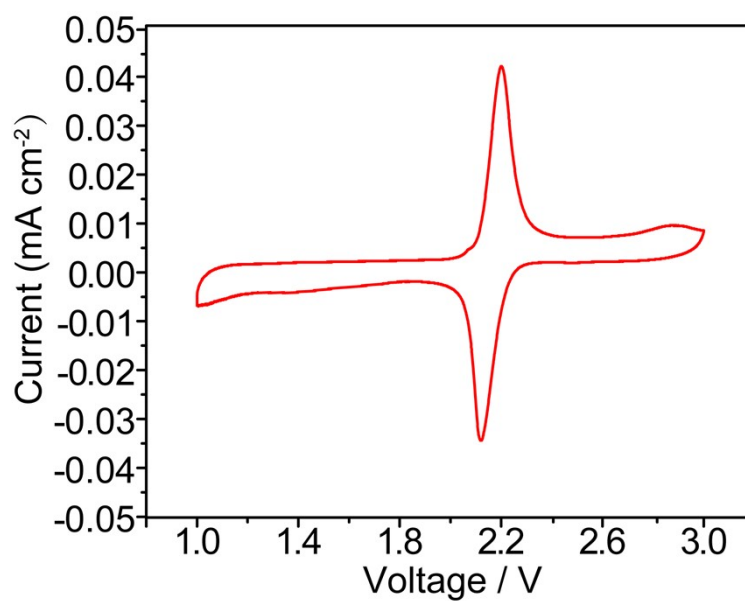


**Fig. S6.** CV curves of the Li|PDSe battery at a scan rate of  $0.1 \text{ mV s}^{-1}$ .

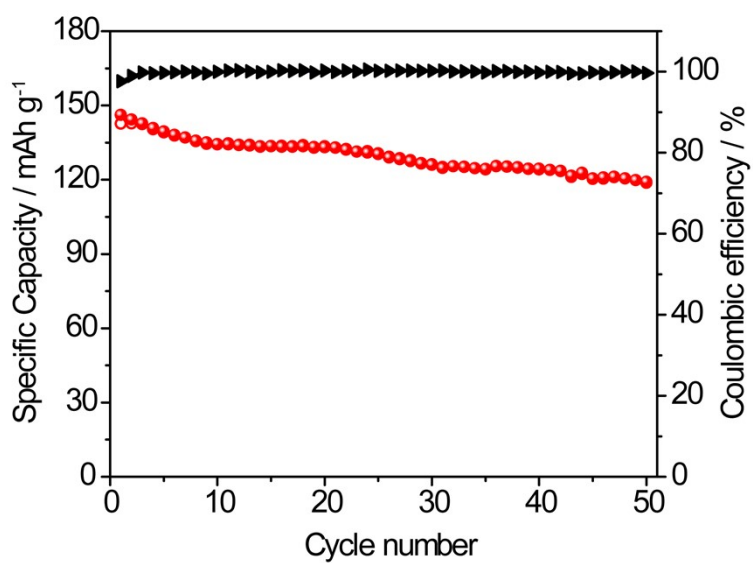


**Fig. S7.** Cycling performance of the Li|PDSe battery at the current densities of 0.5C.

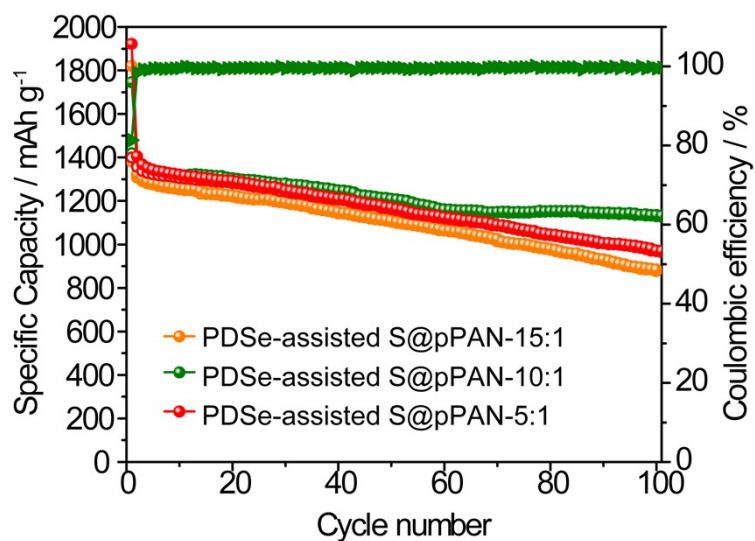


**Fig. S8.** Cycling performances of the Li|S@pPAN batteries under different PDSe concentration at the current densities of 1C in carbonate electrolyte (the molar ratio is S in S@pPAN to Se in PDSe).

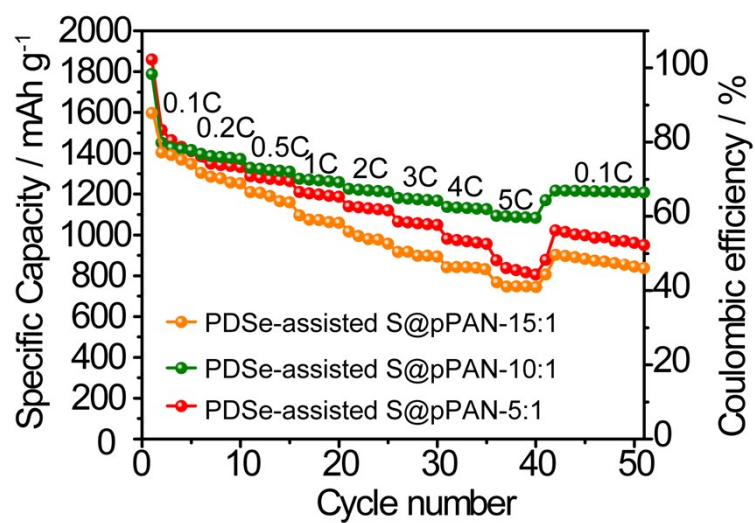


**Fig. S9.** Rate performances of the Li|S@pPAN batteries under different PDSe concentration in carbonate electrolyte (the molar ratio is S in S@pPAN to Se in PDSe).

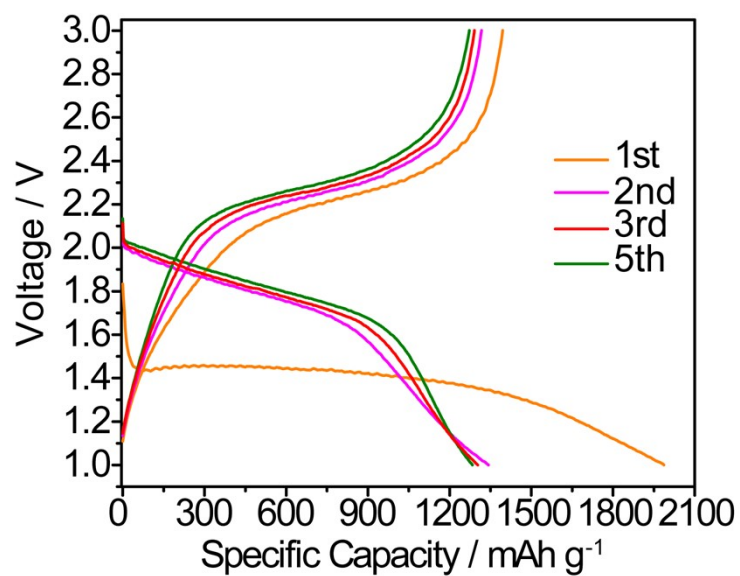


**Fig. S10.** Galvanostatic discharge–charge profiles of the Li|PDSe-assisted S@pPAN battery in the initial five cycles at 0.5C in the carbonate electrolyte.

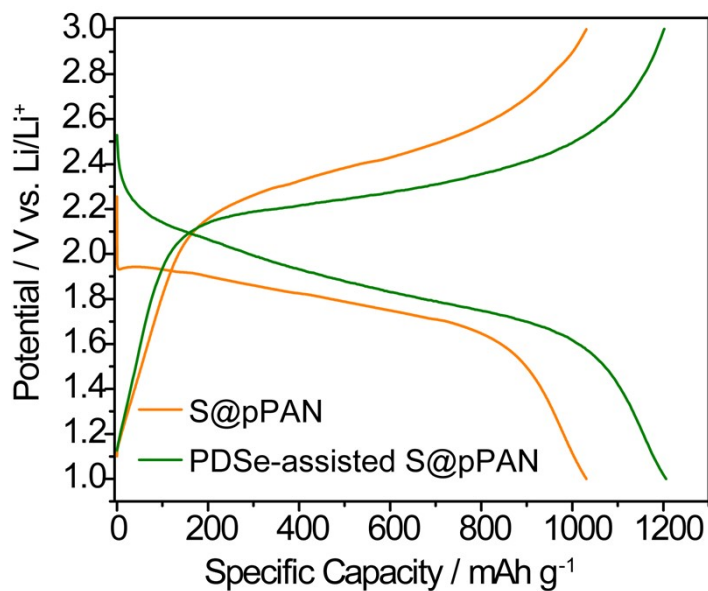


**Fig. S11.** Galvanostatic discharge–charge profiles at the 50<sup>th</sup> cycle of the Li|S@pPAN batteries with/without PDSe at 1C in the carbonate electrolyte.

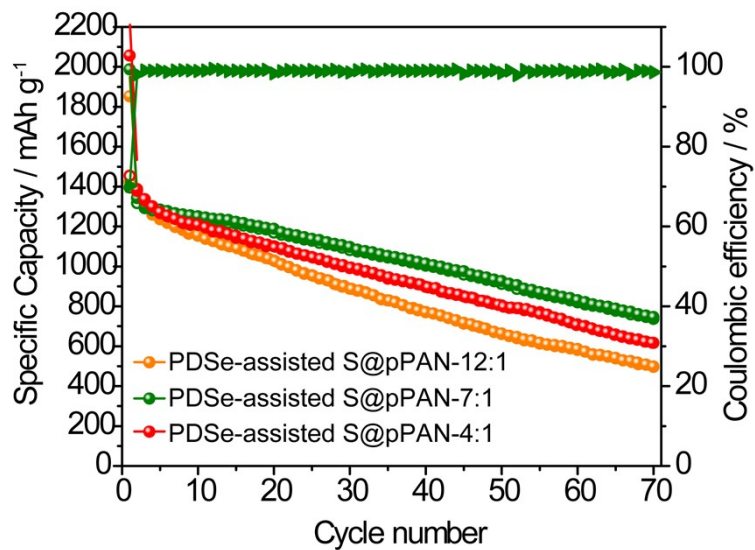


**Fig. S12.** Cycling performances of the Li|S@pPAN batteries under different PDSe concentration at the current densities of 0.5C in ether electrolyte (the molar ratio is S in S@pPAN to Se in PDSe).

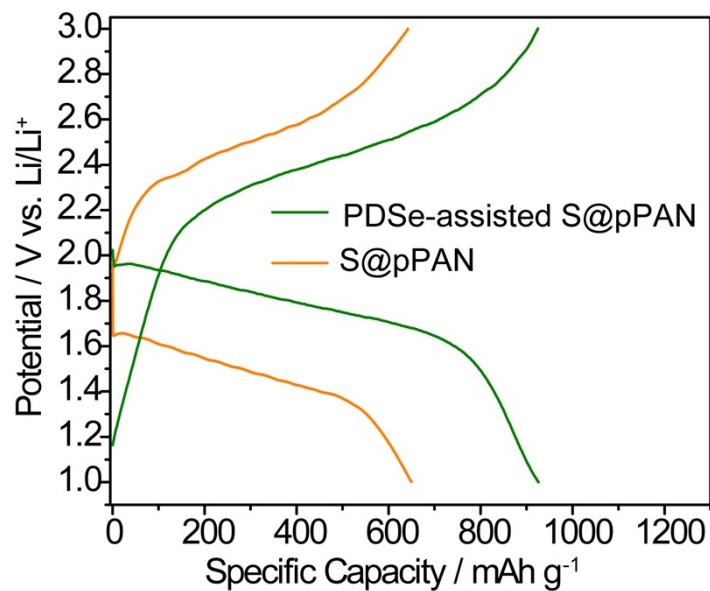


**Fig. S13.** Galvanostatic discharge-charge profiles at the 50<sup>th</sup> cycle of the Li|S@pPAN batteries with/without PDSe at 0.5C in the ether electrolyte.

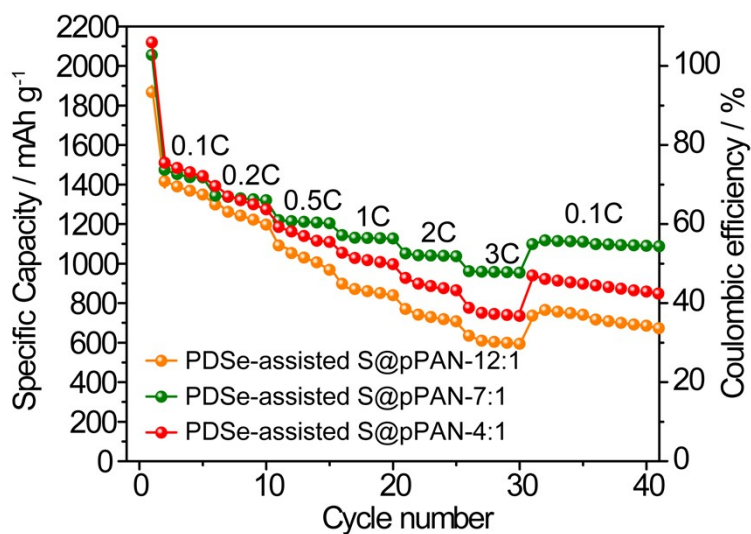


**Fig. S14.** Rate performances of the Li|S@pPAN batteries under different PDSe concentration in ether electrolyte.

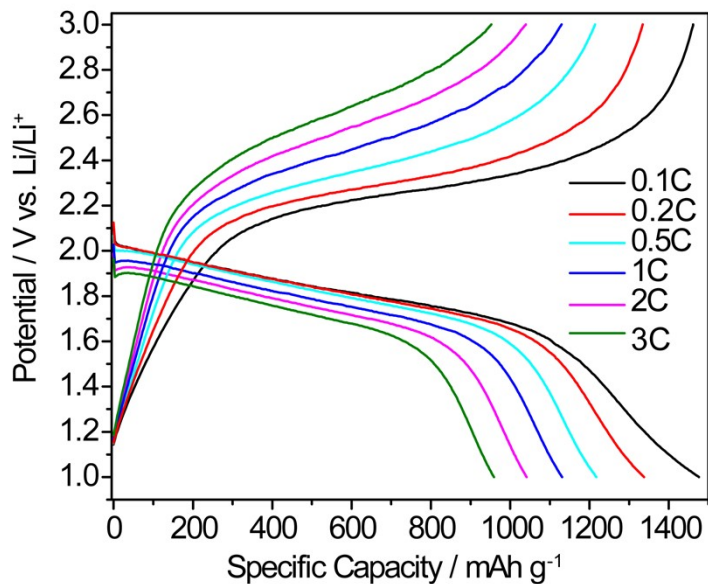


**Fig. S15.** Galvanostatic discharge-charge profiles of the Li|PDSe-assisted S@pPAN battery at different current densities in the ether electrolyte.

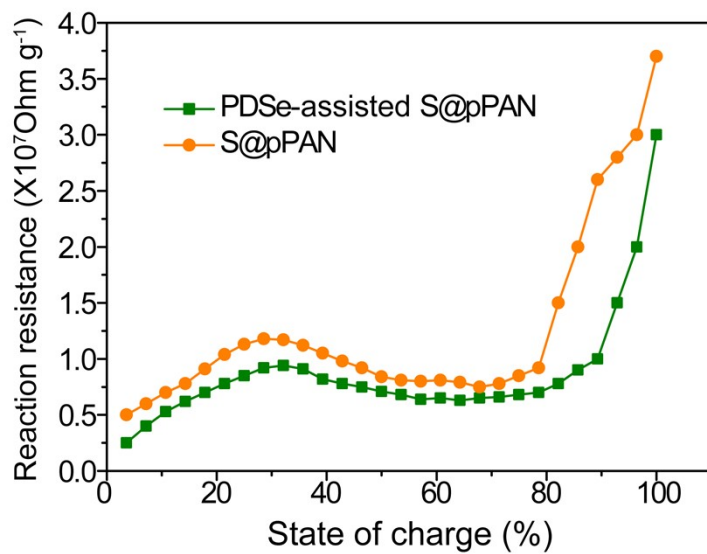


**Fig. S16.** Reaction resistance comparison of the S@pPAN cathodes with/without PDSe during charge process.

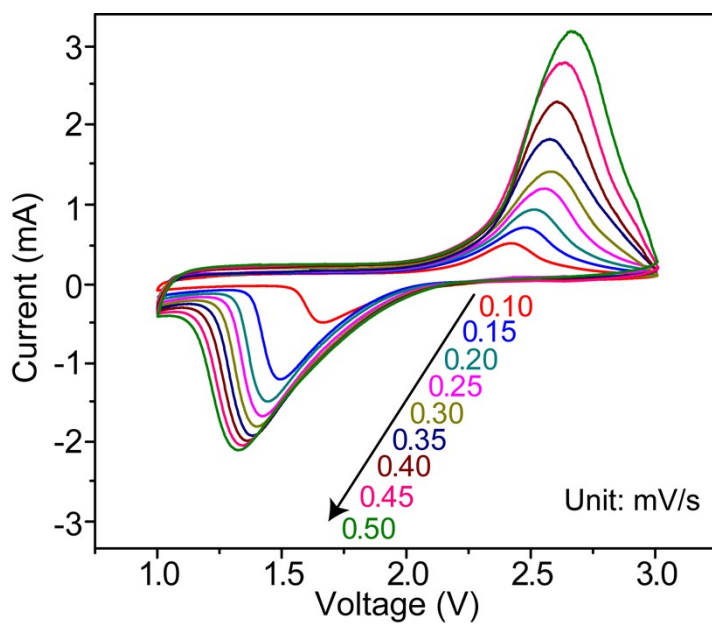


**Fig. S17.** CV curves of the Li|S@pPAN battery at different scan rates.

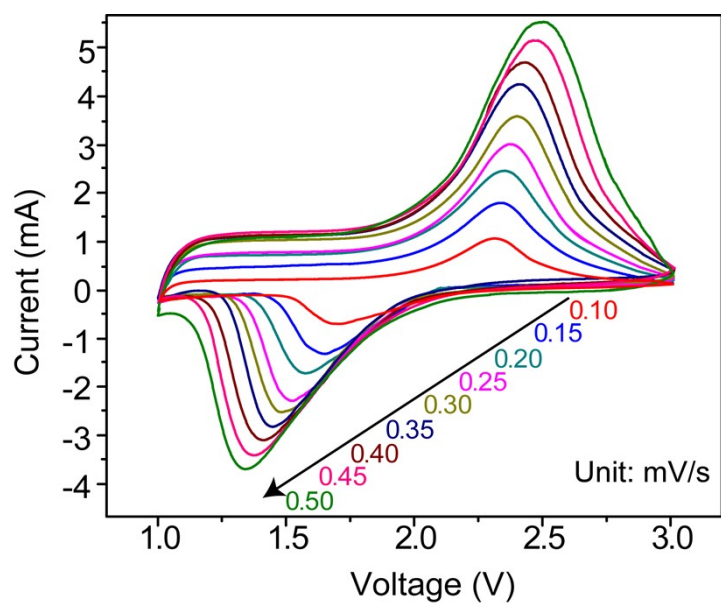


**Fig. S18.** CV curves of the Li|PDSe-assisted S@pPAN battery at different scan rates.

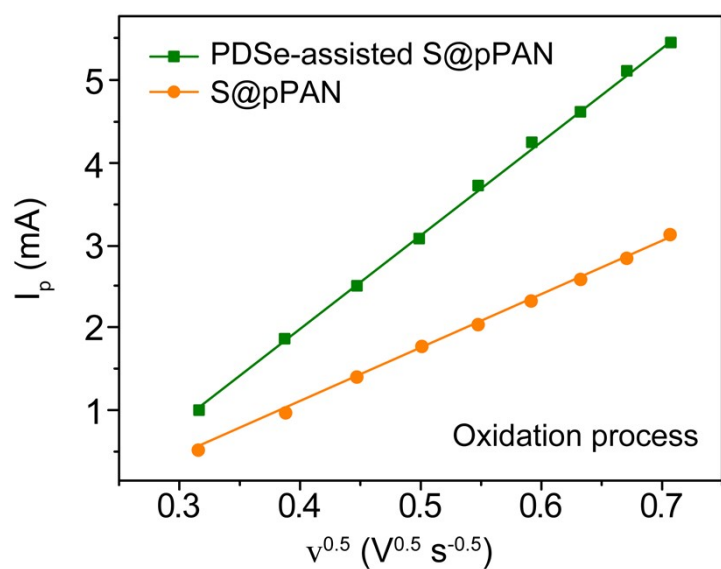


**Fig. S19.** Linear fit profiles obtained from oxidation peaks of CV test at various scanning rates for the Li|PDSe-assisted S@pPAN battery.

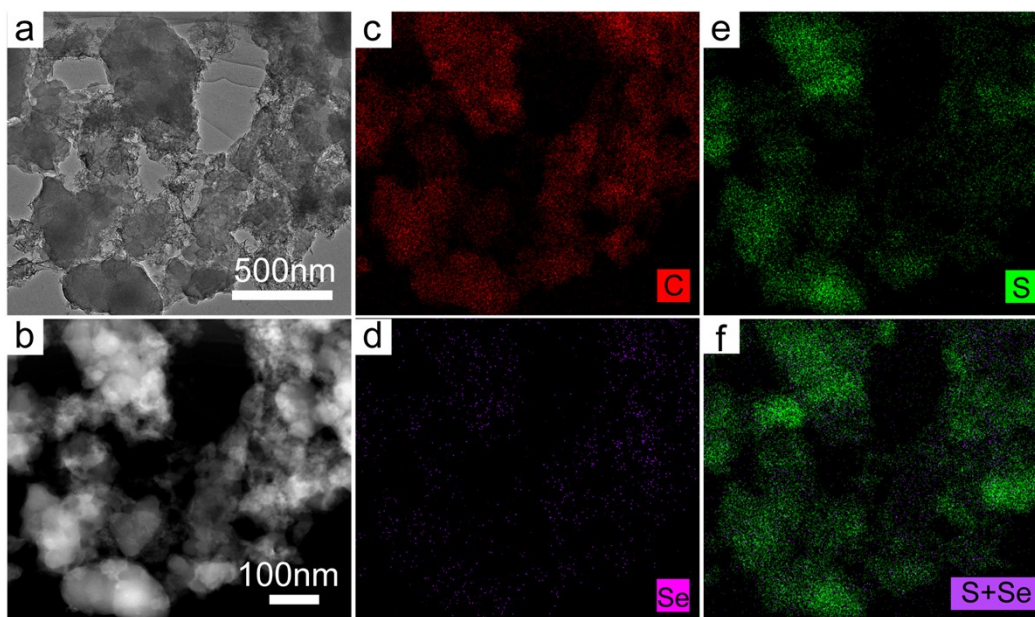


**Fig. S20.** HR-TEM images (a-b) and EDS elemental mapping images of the PDSe-assisted S@pPAN cathode after cycled for C (c), S (d), Se (e) and overlap of S and Se (f).

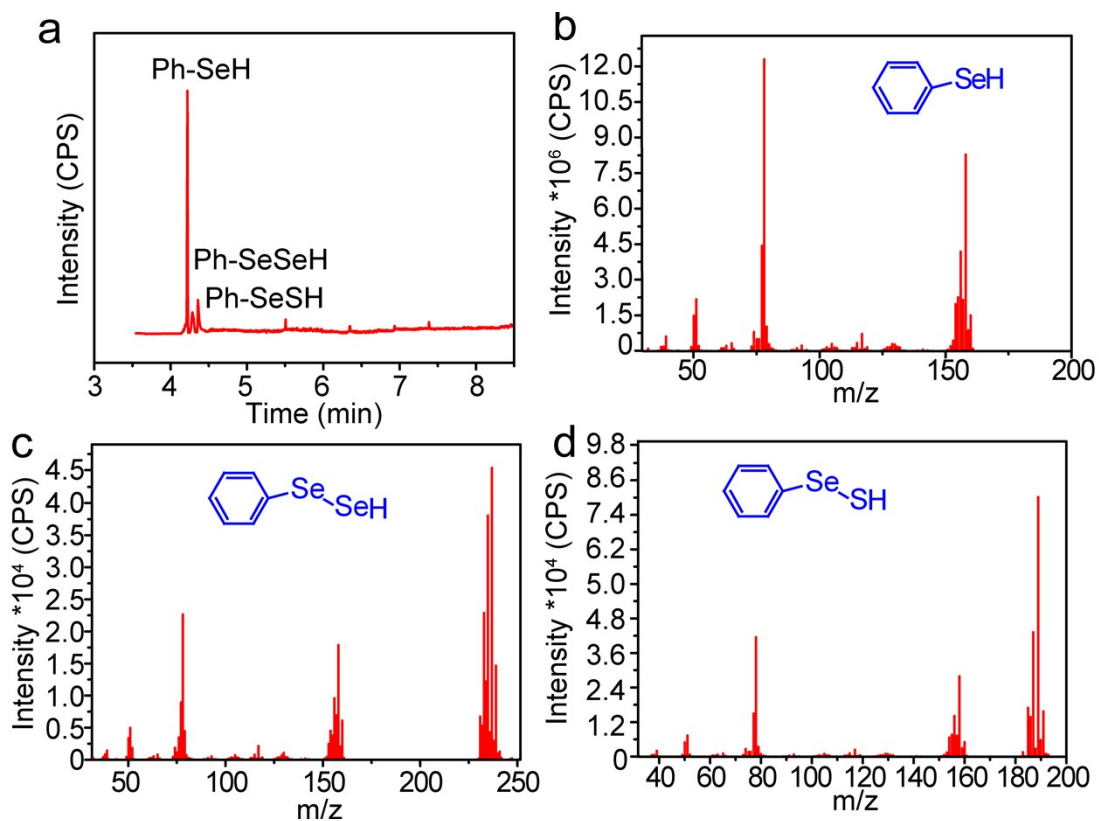


**Fig. S21.** (a) TIC spectrum of the Li|PDSe-assisted S@pPAN battery in ether electrolyte after three cycle at the discharged state, and corresponding discharge products in (b-d).

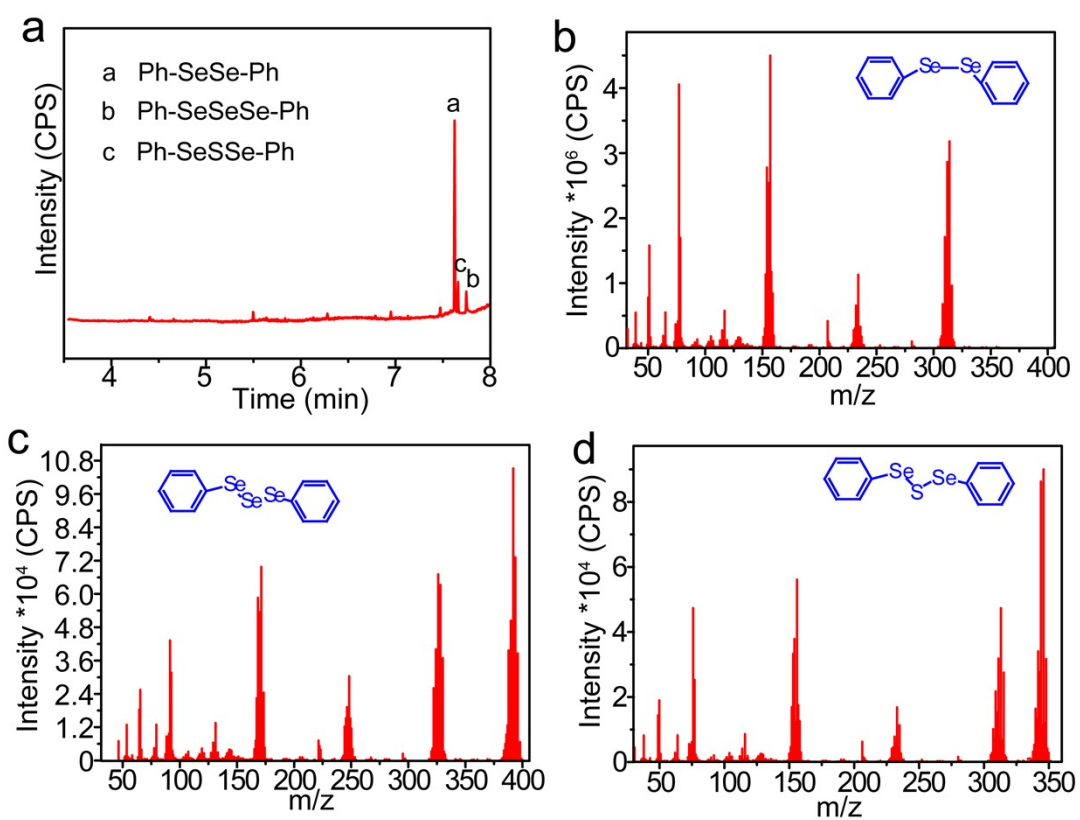


**Fig. S22.** (a) TIC spectrum of the Li|PDSe-assisted S@pPAN battery in ether electrolyte after three cycle at the charged state, and corresponding discharge products in (b-d).

### 3. Supplementary References

- [1] J. Wang, J. Yang, J. Xie, N. Xu, *Adv. Mater.* 14 (2002) 963–965.  
 [2] S. Y. Wei, L. Ma, K. E. Hendrickson, Z. Y. Tu, L. A. Archer, *J. Am. Chem. Soc.* 137 (2015) 12143–12152.